ISBN: 978-3-95450-227-1 ISSN: 2673-5490 doi:10.18429/JACoW-IPAC2022-MOPOPT054

A MODIFIED NOMARSKI INTERFEROMETER TO STUDY SUPERSONIC GAS JET DENSITY PROFILES

C. Swain*, J. Wolfenden, A. Salehilashkajani, H. D. Zhang, O. Apsimon, C. P. Welsch,
Cockcroft Institute and University of Liverpool, Warrington, Cheshire

Abstract

Gas jet-based non-invasive beam profile monitors, such as those developed for the high luminosity Large Hadron Collider (HL-LHC) upgrade, require accurate, high resolution methods to characterise the supersonic gas jet density profile. This paper proposes a modified Nomarski interferometer to non-invasively study the behaviour of these jets, with nozzle diameters of 1 mm or less in diameter. It discusses the initial design and results, alongside plans for future improvements. Developing systems such as this which can image on such a small scale allows for improved monitoring of supersonic gas jets used in several areas of accelerator science, thus allowing for improvements in the accuracy of experiments they are utilised in.

INTRODUCTION

The beam gas curtain (BGC) under development by the Cockcroft Institute, CERN, and GSI utilises a supersonic gas jet to monitor the beam with minimal invasiveness [1] [2]. The main working principles of this monitor which are being tested are ionisation and fluorescence [3]; the signal intensity produced by both of these processes are proportional to the density of the gas jet. Therefore, this a priori characterisation of the gas jet density profile is critical to the operation of a BGC and its behaviour must be studied. For this purpose, a modified Nomarski interferometer [4] has been designed to conduct non-invasive interferometric imaging. The entire optical system has been constructed on a single optical path, which connects directly to the outside of the vacuum chamber. The Nomarski style was chosen due to the single laser path, reducing the system size and chance of calibration errors. This specific design utilises a Wollaston prism to create the interferogram [5]. Following initial calibration, single shot measurements can be analysed instantly using a standard Fourier analysis methodology [6, 7]. This paper presents the design and set up of the current interferometer, alongside initial images, limitations, and planned improvements for the system.

INTERFEROMETRY THEORY

The modified Nomarski interferometer used for this design utilises a Wollaston prism, two triangular prisms made of birefringent material which create a polarising beam splitter when placed together [8]. The two sections are oriented such that the optical axes are perpendicular. A beam hitting the prism and crossing the boundary between the two halves diverges into an ordinary and extraordinary ray with orthogonal polarisations. As the two beams are from a single point source, they are coherent and therefore capable of interference. Interferometers utilise this interference to generate images (or interferograms) which show changes in phase shift that have occurred to the waves.

The phase shift of a light wave propagating through a material is caused by the change in the effective refractive index it experiences. The Lorentz-Lorentz equation states that for gases with a refractive index (η) close to 1, the number density is related via Eq. (1) [9].

$$\rho \approx (\eta - 1)\frac{2}{3}\frac{N_A}{A} \tag{1}$$

where the density is given in cm^{-3}, N_A is Avogadro's constant ($6.022 \times 10^{23}\ \mathrm{mol}^{-1}$), and A is the molar refractivity (for nitrogen, $A = 4.46\ \mathrm{cm}^3\ \mathrm{mol}^{-1}$ [10]). This equation can then be used to show how the phase shift is directly dependant on the density of the gas flow [5]:

$$\Delta\phi = l\frac{3\pi}{\lambda}\frac{A}{N_A}\rho \tag{2}$$

where λ is the laser wavelength and l is the laser path length through the gas jet, in this case taken as equal to the nozzle throat. As the density and phase shift are linked, interferograms can therefore be used to calculate the changing density profile of a gas jet.

EXPERIMENTAL SET UP

Figures 1 and 2 show the components of the interferometer system before and after the chamber. In Fig. 1, a 532 nm laser propagates through a linear polariser and beam expander before passing through the chamber. A 10x beam expander was introduced to the set up as the Gaussian profile of the laser caused changes in intensity, which created irregularities at the edges of the interferograms, affecting the accuracy of the results. In Fig. 2, after the chamber, an achromatic doublet lens with a focal length of 150 mm focused the laser onto a CMOS camera. The lens also provided a magnification factor of 2. The Wollaston prism was adjustable across a range of 180 mm to allow for fringe spacings (δ_f) to be altered, as shown in Eq. (3) [11].

$$\delta_f = \frac{\lambda b}{\epsilon a} \tag{3}$$

where λ is the wavelength of the laser, ϵ is the separation angle of the Wollaston prism, b is the distance between the prism and the imaging plane (in this case the CMOS), and a is the distance between the focusing lens and the prism. The secondary polariser was set orthogonal to the first. This meant that any light from the laser which was not refracted

* Catherine.Swain@liverpool.ac.uk

ISBN: 978-3-95450-227-1 ISSN: 2673-5490 doi:10.18429/JACoW-IPAC2022-MOPOPT054

by the gas jet would be attenuated before reaching the CMOS, thus reducing noise in the resulting images. All optics were contained in a cage system to ensure the alignment remained stable.

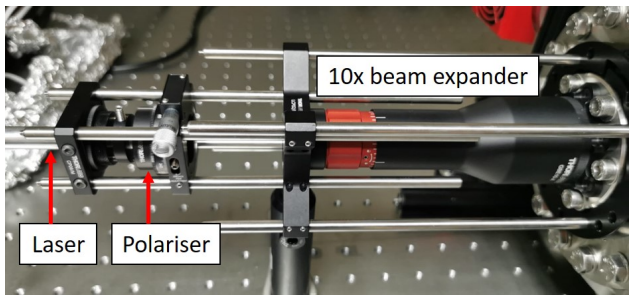

Figure 1: Interferometer components before the vacuum chamber, from left to right: 532 nm laser, linear polariser, 10x magnification beam expander.

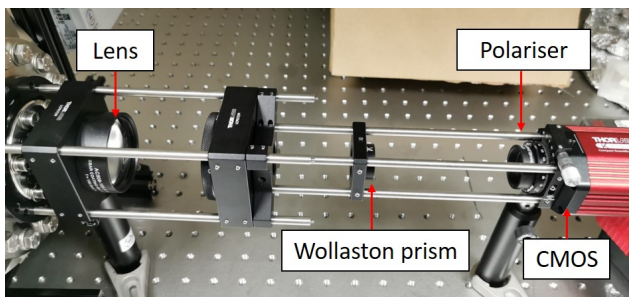

Figure 2: Interferometer components after the chamber, from left to right: 150 mm focal length lens, Wollaston prism, polariser, CMOS.

The system used interchangeable nozzle diameters ranging from 30 µm to 1 mm to allow for testing across a range of gas jet sizes. The nozzle was housed inside the vacuum chamber on a 3D translation stage, meaning alignment of the system was simple and could be done externally after the optics had been fitted. Nitrogen gas was used for the jet due to its usage in the BGC development, although argon was also considered for its higher density. The gas jet was operated using a solenoid valve, and its runtime was between 0.1 and 1.75 s. Due to the small vacuum chamber chosen for this set up, operating the gas jet for longer than this reduced the pressure differentials important for this diagnostic. The short runtime of gas did not have adverse effects on the process however, as images were all taken with a low exposure time (< 1 ms). The chamber was capable of sustaining a vacuum up to 10^{-8} mbar although with repeated use of the gas jet it rose to 10^{-6} mbar , therefore this was considered the backing pressure for calculations.

INITIAL RESULTS AND DISCUSSION

Figure 3 shows the interference fringes created by the Wollaston prism as imaged when positioned 175 mm from the CMOS. As shown in Eq. (3), fringe spacing is proportional to the distance between these two components [12], and in this case is 55.2 µm. This would provide 153 fringes across the interferogram, however the inclusion of the nozzle on the left of the image means only 128 fringes are available for viewing the phase shift.

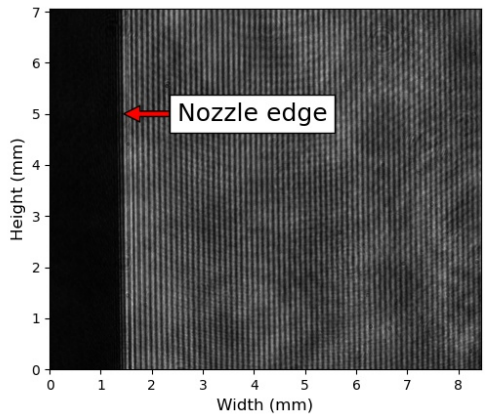

Figure 3: Interferogram produced with a Wollaston prism with the nozzle indicated on the left, fringe spacing of 55.2 µm.

The CMOS size is 2048x2440 pixels, which each pixel measuring 3.45 x 3.45 µm (Δ). Given the chip and pixel size, alongside an assumption of 5 fringes providing the detail necessary to image phase shift, the maximum fringe width (δ_f) was calculated. From this value, the minimum phase shift ($\Delta\phi_{min}$) that the system had the capability to be measured using Eq. (4).

$$\Delta\phi_{min} = 2\pi\frac{\Delta}{\delta_f} = 12.8\,\text{mrad} \tag{4}$$

As discussed previously, phase shift is caused by the changes in density. Therefore, in order to determine whether the optics are capable of measuring the changes in phase shift, the estimated longitudinal density profile of the gas jet was calculated. Using the phase shift found in Eq. (4), the minimum density necessary to induce a measurable phase shift was found. Equation (5) gave the density profile for a distance of 2000 µm from the nozzle throat [5], as shown in Fig. 4.

$$\rho \approx 0.15\rho_0\left(\frac{0.74d}{x\tan\theta}\right)^2 \tag{5}$$

The number density before the nozzle (ρ_0) is found through the ideal gas law, using a range of gas jet pressures (0.5 – 2 bar). The diameter of the nozzle throat (d) and the half angle of the nozzle (θ) were 30 µm and 45° respectively. The distance from the nozzle throat (x) was varied to produce the graphs.

Figure 4 shows the density decreases exponentially, with each plot reducing by 83.3 - 83.6% within the first 250 µm from the nozzle. The phase shifts given in Fig. 5 show how this is proportional to the density, decreasing at the same rate. The minimum phase shift resolution of the system is

ISBN: 978-3-95450-227-1 ISSN: 2673-5490 doi:10.18429/JACoW-IPAC2022-MOPOPT054

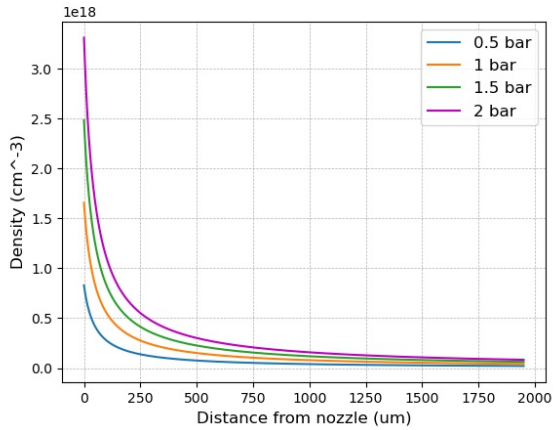

Figure 4: Calculated longitudinal density profile for 0.5, 1, 1.5, and 2 bar gas jets across a 2000 µm range from the nozzle throat.

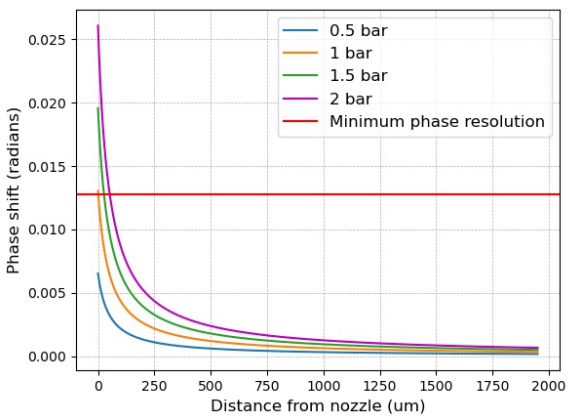

Figure 5: Estimated phase shifts for the gas jets from Fig. 4 with the minimum visible phase resolution in red.

shown as a horizontal red line at 12.8 mrad. Any phase shift below this value cannot be recorded, therefore neither the 0.5 nor the 1 bar gas jets would be a feasible choice for this system; the first only reaches half the necessary phase shift and the second only achieves this value for $x < 0.8$ µm. The 1.5 and 2 bar jets are both greater than this value for a larger distance, 26 µm and 51 µm respectively.

This analysis of the phase shifts shows that a higher pressure gas jet is necessary for an interferogram to be imaged, however this introduces experimental issues. Due to the size of the chamber and position of the turbomolecular pump used in the current set up, high pressures can cause the vacuum-to-gas jet pressure gradient to drop to a level which is no longer appropriate for interferometry. Additionally, as the area within which the phase shift can be detected is in the order of micrometres, imaging with the current set up would prove challenging. Therefore, upgrades to the design have been planned, the main focus of which being the integration of a microscope system. This will allow for imaging much smaller areas of the gas jet and provide a means of focusing the phase shift resolution of this system in these important areas.

CONCLUSIONS

This contribution has described the design of a modified Nomarski interferometer intended for use in monitoring the density profiles of supersonic gas jets. Use of a Wollaston prism and equations governing the relationship between density changes and measurable phase shift were presented. The current experimental set up has been shown, as was a resulting initial interferogram with a fringe spacing of 55.2 µm. Minimum phase resolution of the imaging components was calculated as 12.8 mrad. Limitations of the system were discussed and while it was shown that results could be gained, the decision to make upgrades before proceeding with data collection were explained. In order to gain accurate images within the 26 – 51 µm containing large enough phase shift to measure, a microscope will be incorporated into the interferometer to improve the phase shift resolution of the required small fringes.

ACKNOWLEDGEMENTS

This work is supported by the AWAKE-UK phase II project grant No. ST/T001941/1, the STFC Cockcroft core grant No. ST/G008248/1 and the HL-LHC-UK phase II project funded by STFC under Grant Ref: ST/T001925/1.

REFERENCES

[1] V. Tzoganis, H. D. Zhang, A. Jeff and C. P. Welsch, "Design and first operation of a supersonic gas jet based beam profile monitor", *Phys. Rev. Accel. Beams*, vol. 20, p. 062801, 2017. doi:10.1103/PhysRevAccelBeams.20.062801

[2] H. D. Zhang *et al.*, "Development of Supersonic Gas-Sheet-Based Beam Profile Monitors", in *Proc. IPAC'19*, Melbourne, Australia, May 2019, pp. 2717–2720. doi:10.18429/JACoW-IPAC2019-WEPGW096

[3] A. Salehilashkajani *et al.*, "A gas curtain beam profile monitor using beam induced fluorescence for high intensity charged particle beams", *Applied Physics Letters*, vol. 120, p. 174101, 2022. doi:10.1063/5.0085491

[4] M. Kalal, O. Slezak, M. Martinkova and Y. J. Rhee, "Compact Design of a Nomarski Interferometer and Its Application in the Diagnostics of Coulomb Explosions of Deuterium Clusters", *Journal of the Korean Physical Society*, vol. 56, no. 1, pp. 289-294, 2010.

[5] A. Adelmann *et al.*, "Real time tomography of gas jets with a Wollaston interferometer", *Appl. Sci.*, vol. 8, p. 443, 2018. doi:10.3390/app8030443

[6] J. M. Cole, "Diagnosis and Application of Laser Wakefield Accelerators", Ph.D. thesis, Phys. Dept., Imperial College London, London, England, 2016.

[7] Q. Liu *et al.*, "Application of Nomarski interference system in supersonic gas-jet target diagnosis", *AIP Advances*, vol. 11, p. 015145, 2021. doi:10.1063/5.0027317

ISBN: 978-3-95450-227-1 ISSN: 2673-5490 doi:10.18429/JACoW-IPAC2022-MOPOPT054

[8] E. Hecht, *Optics* , MA, USA: Addison Wesley Longman Inc, 2002.

[9] Y. Liu and P. H. Daum, "Relationship of refractive index to mass density and self-consistency of mixing rules for multicomponent mixtures like ambient aerosols", *Journal of Aerosol Science*, vol. 39, no. 11, pp. 974-986, 2008. doi:10.1016/j.jaerosci.2008.06.006

[10] A. D. Buckingham and C. Graham, "The Density Dependence of the Refractivity of Gases", in *Proc. R. Soc. Lond. A*, vol. 337, pp. 275-291, 1974. doi:10.1098/rspa.1974.0049

[11] S. S. Harilal and M. S. Tillack, "Laser plasma density measurements using interferometry", University of California, San Diego, USA, UCSD-ENG-114, Oct. 2004.

[12] A. Howard, D. Haberberger, R. Boni, R. Brown, and D. H. Froula, "Implementation of a Wollaston interferometry diagnostic on OMEGA EP", *Rev. Sci. Instrum.*, vol. 89, p. 10B107, 2018. doi:10.1063/1.5036956